THE JOURNAL OF PHYSICAL CHEMISTRY B LETTERS

2005, *109,* 24−26
Published on Web 12/16/2004

Adsorbate-Geometry Specific Subsurface Relaxation in the CO/Pt(111) System

J. X. Wang,*,† I. K. Robinson,‡ B. M. Ocko,§ and R. R. Adzic†

Materials Science Department, Brookhaven National Laboratory, Upton, New York 11973, Department of Physics, University of Illinois at Urbana-Champaign, Urbana, Illinois 61801, and Physics Department, Brookhaven National Laboratory, Upton, New York 11973

Received: October 28, 2004; In Final Form: November 23, 2004

A dramatic multilayer substrate relaxation is observed for the ($\sqrt{19}\times\sqrt{19}$)-13CO adlayer phase on a Pt(111) electrode by surface X-ray scattering. Within the ($\sqrt{19}\times\sqrt{19}$) unit cell, a vertical expansion of 0.28 Å was determined for the Pt atoms under near-top-site CO molecules, whereas only 0.04 Å was found under near-bridge-site CO molecules. The lateral displacements involve small rotations toward more symmetric bonding. Both the expansions and rotations extend into the bulk with a decay length of 1.8 Pt layers. This nonuniform layer expansion, hitherto unseen, appears to be a manifestation of the differential stress induced by CO adsorption at different sites.

Rich structural behavior involving surface relaxation (displacements from bulk lattice sites) or reconstruction (changes of the in-plane unit cell) has been found on a number of substrates, under the influence of adsorption and other environmental factors. On metals, surface electron density plays a major role in determining surface reconstruction, relaxation, and stress.[1−3] On semiconductors, the displacements of surface atoms are more often driven by the predisposition to specific bonding geometry.[4] In this Letter we report a nonuniform layer expansion of the Pt(111) electrode surface induced by the ($\sqrt{19}\times\sqrt{19}$)-13CO adlayer, presumably due to the localized charge in the molecule-metal bonds that varies with adsorption site.

In recent years, scanning tunneling microscopy (STM) has revealed the phase behavior of the CO adsorption on Pt(111) at both electrochemical[5] and gas/solid[6] interfaces. In both cases, a high-order commensurate ($\sqrt{19}\times\sqrt{19}$) unit cell containing 13 CO molecules was observed. The notable differences in height between the CO molecules at different adsorption sites were attributed to the differences in CO−Pt spacing, not to any substrate relaxation. Surface X-ray scattering techniques, which offer the necessary penetration for studying subsurface, have been employed in studies of CO adsorption on metal surfaces at both gas/solid[7] and solution/electrode interfaces.[8] In the present study, we discovered a new type of substrate relaxation, viz., a profound multilayer surface relaxation with nonuniform layer expansion. Its physical origin has implications for a better understanding of CO adsorption energetics, which have been intensively studied by density functional theory (DFT) and various experimental techniques.[9]

The Pt(111) crystal was prepared by flame annealing and cooling in Ar/H_2 mixed-gas flow until a drop of electrolyte could be placed on its surface to prevent direct contact with air. The electrochemical cell was sealed by an X-ray window film, which allows CO gas to diffuse from an outer chamber into the solution (either 0.05 M H_2SO_4 or 0.1 M $HClO_4$). X-ray measurements were taken using focused X-rays ($\lambda = 1.2$ Å) at beam line ×22A at the National Synchrotron Light Source. Following convention, we used a hexagonal coordination system to index the Pt(111) crystal, in which $q = (a^*, b^*, c^*)\cdot(H, K, L)$, where $a^* = b^* = 4\pi/\sqrt{3}a$, $c^* = 2\pi/\sqrt{6}a$, and $a = 2.775$ Å. A 2 × 2-mm detector slit was located 650 mm from the sample. The incident slits were adjusted during the measurements to maintain the illuminated area within the borders of the crystal. The intensities at each (H, K, L) position were determined by integrating the θ-rocking curve and then corrected for the Lorentz factor, active sample area, and change of the resolution function. The intensity data are customarily plotted along "rods" as a function of the continuous variable L with fixed H and K values. The scaling constant used for all the rods was determined by making those at (0,0), (1,0), (0,1), and (1,1) positions measured at open circuit in nitrogen-saturated solution comparable with the calculated curves for a nearly ideally terminated Pt(111). Good agreements between measured and calculated rods showed that in the absence of CO the Pt(111) electrode is free from reconstruction, relaxation, and surface roughness.

Figure 1 shows two distinct ways of forming a ($\sqrt{19}\times\sqrt{19}$)-13CO superlattice structure: they differ by the rotation angle between the lattice axes of the close-packed CO adlayer and substrate. With all the CO molecules at the uniformly spaced lattice sites, both structures can have 1 top-site, 6 near-top-site, and 6 near-bridge-site CO molecules. The "patch"/"ring" model in the top/bottom of the left panel of Figure 1 has six near-top/bridge-site CO molecules surrounding the top-site CO, respectively. The two models are distinguishable by the location of the CO diffraction peaks. The observed pattern, shown by the red circles in the right panel, has the first-order peaks 9.52° from the H and K axes and thus corresponds to the "patch" model, consistent with the STM results[5,6] and that observed by a recent surface X-ray diffraction study.[10] The typical φ rocking curve has a peak width around 0.1°, only slightly larger than the peak width of 0.07° at (0, 1, 0.12), indicating that the domain size is large and the "patch" structure is highly preferred. However, its energetic advantage is not easy to understand without invoking a stabilizing role of the substrate.

Additional diffraction peaks were observed at some allowed positions of the ($\sqrt{19}\times\sqrt{19}$) unit cell, especially strong in the satellites immediately surrounding the integer positions. This

† Materials Science Department, Brookhaven National Laboratory.
‡ University of Illinois at Urbana-Champaign.
§ Physics Department, Brookhaven National Laboratory.

10.1021/jp045082i CCC: $30.25

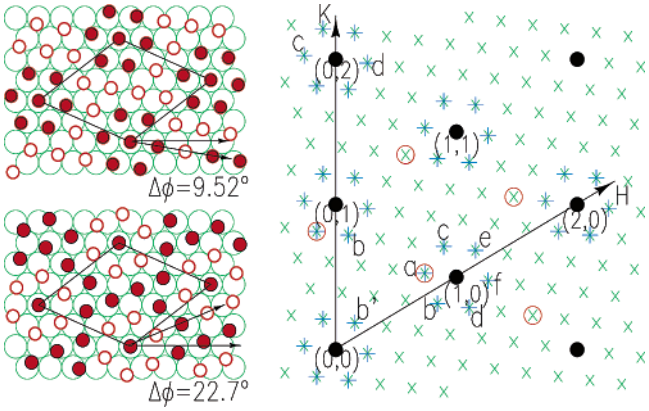

Figure 1. Left panel: Distinct superstructures for the ($\sqrt{19}\times\sqrt{19}$)-13CO monolayer on Pt(111). Open (solid) small circles represent the CO in nearly bridge (top) sites. The one in the top panel, named "patch" model, is the one observed, not the "ring" model in the bottom panel. Right panel: In-plane diffraction pattern corresponding to the ($\sqrt{19}\times\sqrt{19}$) unit cell (green cross). Red circles denote the primary positions of the CO contributions. Blue plus symbols denote the positions of the strong surface relaxation peaks. Labels correspond to the panels of Figure 2.

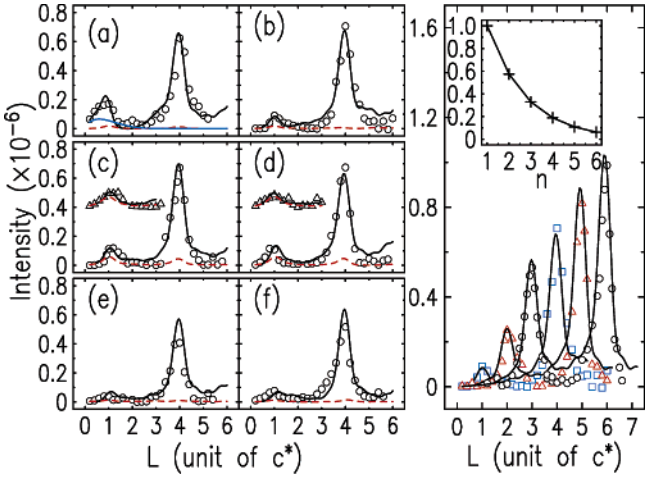

Figure 2. Left panel: Six measured rods (circles) shown in (a) to (f) correspond to the rods surrounding (1, 0) labeled by a−f in Figure 1. The triangles in (c) and (d) (offset on *y*-axes) are the measured c and d rods near (0, 2). The solid (black) and dashed (red) lines are the best fits and that with the vertical displacements excluded, respectively. The solid (blue) line in (a) shows the intensity from the CO molecules. Right panel: The (1, 0)*b* (blue square), (0,1)*b* (red triangles), and (0,0)-*b*′ rods. Solid lines are the best fits ($D_7 - D_{12} = 0.24$ Å and $\tau_z = 1.8$). Inset: Relative displacement amplitude for layer *n*.

pattern, shown in Figure 1 (right panel), is similar to those observed from surface reconstructions[2] and suggests significant displacements of the Pt substrate atoms. When the potential was varied, these diffraction peaks rose and fell in synchrony with the formation of the ($\sqrt{19}\times\sqrt{19}$)-13CO phase. At 0.8 V versus a reversible hydrogen electrode, where measured X-ray intensities were stable with time, we measured 31 independent noninteger rods, including one satellite near the origin and six satellites around each of the five low-integer index positions. The intensity measured from the mirror-equivalent domain was slightly weaker (~85%), so averaged intensities were used for the noninteger rods. As shown in Figure 2 (left panel), two rather sharp peaks were centered at $L = 1$ and 4 in all six satellite rods in the vicinity of (1, 0). Similar peaks were found in all other noninteger rods, where they are centered at $L = 2$ and 5 for the rods near (0, 1) and (2, 0), and at $L = 3$ and 6 for the rods near (0, 0) and (1, 1) following the Bragg positions of the neighboring integer rods. These features clearly indicate a

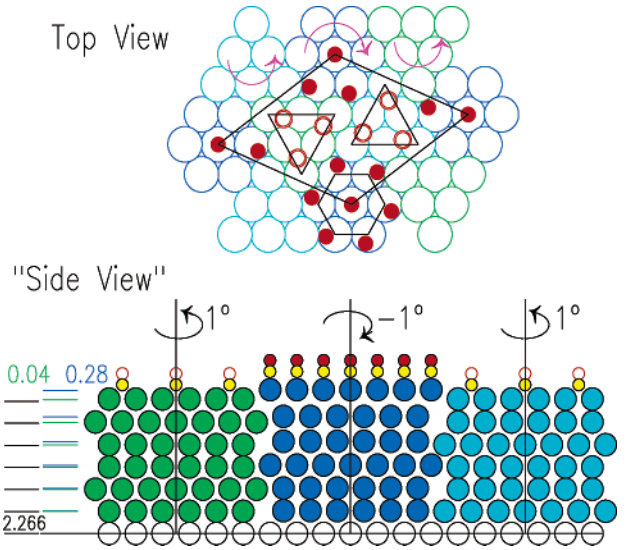

Figure 3. Structural model of the Pt(111) surface relaxation induced by the ($\sqrt{19}\times\sqrt{19}$)-13CO phase. Small solid and open circles represent the CO molecules in nearly top and bridge sites, respectively. Large circles in different colors represent the Pt atoms in three groups with different rotation centers. The "side view" is not a projection, but a simplified picture to illustrate schematically the grouping and layer expansion. The top layer expansions of 0.28 and 0.04 Å from the lattice positions are amplified 4-fold for visibility.

multilayer subsurface relaxation because oscillations in rods occur when more than one layer contributes and more layers cause sharper peaks.[11] Neither these distinctive features nor the high-intensity level can be produced by any CO displacements from ideal lattice sites.

On the basis of these observations, we constructed a three-dimensional structural model that includes 13 CO molecules and 114 Pt atoms in six layers of 19 atoms each. The in-plane positions of the vertically oriented CO molecules (oxygen terminated) were fixed at the adlayer lattice sites using a 1.15 Å CO bond length. The Pt−C layer spacing was found to be 1.85 and 1.45 Å for the 7 COs at on/near top sites and the 6 COs at the near-bridge sites, respectively, consistent with the published data.[12] Figure 3 (top view) shows how the 19 Pt atoms in the top-layer of the ($\sqrt{19}\times\sqrt{19}$) unit cell are grouped into a motif that contains 7 Pt atoms in a centered-hexagon and 12 Pt atoms that are split between two triangular regions. Within each group, the Pt atoms are allowed to expand/contract laterally and to rotate around their center. Along the surface-normal direction, the displacements of the topmost Pt atoms are controlled by two parameters: D_7 for the 7 Pt atoms under the 7 on/near top site CO molecules and D_{12} for the 12 Pt atoms under the 6 near-bridge site CO molecules. For the underlying layers, the Pt atoms are assigned to either a centered-hexagon or a triangular region based on the ABC stacking sequence. This feature is illustrated schematically by the simplified "side view" shown in Figure 3. The Pt displacements from their ideal positions in the next 5 underlying layers are assumed to follow a simple exponential decay function with characteristic depths, τ_z and τ_{xy}, e.g., for the *n*th layer $D_7(n) = D_7 \exp(-(n-1)/\tau_z)$.

The increase in intensities at larger L in all the noninteger rods, shown in Figure 2, manifests the differences in the vertical displacements of the Pt atoms because the intensities originated from any in-plane displacements do not increase with increasing L, and further, a uniform layer expansion/contraction has no effect on these noninteger rods. The right panel of Figure 2 displays the three satellite rods with the lowest in-plane vectors that have peaks at different L from 1 to 6. The best fits to these

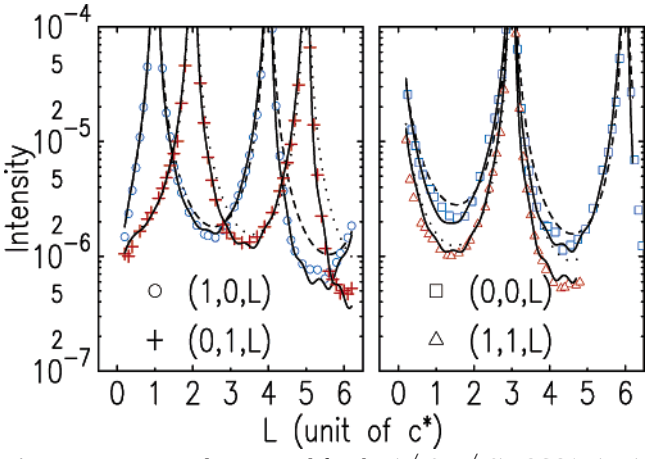

Figure 4. Integer rods measured for the ($\sqrt{19}\times\sqrt{19}$)-13CO/Pt(111) phase. The dotted and dashed lines are the curves measured for ideally terminated Pt(111) in the absence of CO. The solid lines are the best fits with $D_7 = 0.28$, $D_{12} = 0.04$ Å, and $\tau_z = 1.8$ layers.

rods yield $D_7 - D_{12} = 0.24 \pm 0.03$ Å with $\tau_z = 1.8 \pm 0.3$ layers. Note that these values were determined with the scaling factor constrained by the intensities measured for the crystal truncation rods as described earlier in the Experimental Section. The uncertainties given are due to the coupling of the two parameters, i.e., a small decrease in the splitting of the top layer, $D_7 - D_{12}$, can be compensated by a small increase of the depth of the relaxed layers. The root-mean-square (rms) displacement amplitudes in Debye−Waller factor for the Pt surface layers, σ_{xy} and σ_z, were both 0.09 ± 0.1 Å, only slightly larger than that of the bulk Pt crystal (0.08 Å). For $\tau_z = 1.8$, as shown in the insert of Figure 2 (right panel), the displacements for the third and sixth layers dropped to 33 and 6% of those for the top layer, respectively.

The crystal truncation rods at low integer positions were measured to determine the absolute values of D_7 and D_{12} in relation to the normal position of the lattice. As shown in Figure 4, the intensities rise and fall at the lower and higher sides of the Bragg positions, compared with an ideally terminated Pt(111) surface in the absence of CO. These changes indicate that the overall vertical displacement is expansion. The best fits yield $D_7 = 0.28$ Å, $D_{12} = 0.04$ Å, $\tau_z = 1.8$, and $\sigma_z = \sigma_{xy} = 0.09$ Å, consistent with the results of noninteger rods.

In fine-tuning the fits for all the noninteger rods, small in-plane rotations had to be made to produce the observed peaks at small L and large in-plane vectors, where the intensities are most sensitive to in-plane displacements. Two representative peaks are shown in Figures 2c,d. The intensity contribution from the in-plane rotations shown by the red dashed lines is nearly the same as that including both in-plane and vertical displacements shown by the black solid lines for the two rods near (0, 2). The fitting analysis gives a −1° rotation (clockwise) for the Pt atoms in the hexagon under the near-top-site COs and a +1° rotation (counterclockwise) for those in the two triangles under the near-bridge-site COs with the τ_{xy} fixed at 1.8 (solid lines). The uncertainty of ±0.3° is related to the uncertainty of τ_{xy} in a small range similar to the case for τ_z discussed earlier. Last, the "a" type rods (see Figure 1) were analyzed to determine the CO−Pt spacing (values given in the earlier discussion on the model) and rms amplitudes of the CO adlayer. The blue line in Figure 2a shows the intensity contribution from the CO adlayer. The lateral rms amplitude for CO was found rather large, $\sigma_{xy} = 0.3 \pm 0.1$ Å, compared with $\sigma_z = 0.1 \pm 0.1$ Å along the surface-normal direction. The large σ_{xy} value is consistent with that determined from the intensity ratio for the second- and third-order CO peaks. This finding is not surprising because the reported value for CO on Pd(100)[13] is 0.45 Å. Because good fits were obtained for all the rods without lateral expansion, we conclude that the in-plane relaxation involves only small rotations toward more symmetric CO−Pt bonds.

To rationalize the observed subsurface relaxation, we note that a crucial role is played by the nonuniform stress created by the adsorption of CO. Using ab initio cluster models[14] to analyze the bonding mechanism for CO adsorption on Pt(111), the net charge transfers due to excess electron back-donation from Pt to CO were found to be −0.240 and −0.214 electron for a CO molecule adsorbed on the top and at the bridge sites, respectively. Because there is one Pt atom per CO for the on/near top sites and two for the near-bridge sites (see the model in Figure 1 or 3), the partial positive charge on Pt would be 0.240 and 0.107 per atom, respectively. Because these "charges" are due to the polarization in localized CO−Pt bonds, they result in nonuniform stress that closely follows the adsorption-geometry-specific pattern. The energy advantage for having near-top-site COs surrounding the top-site COs in the "patch" model becomes apparent because these Pt atoms can expand to the same height with fewer lattice mismatch boundaries than in the "ring" model where they are separated by the near-bridge-site CO molecules. Furthermore, the "patch" structure is more favorable for the extension of relaxation into deeper layers. When the layers are split, in-plane rotation can occur with less mismatch resistance at the boundaries. Collectively, the multilayer relaxation occurs, which, in turn, makes the "patch" lattice structure preferred over the "ring" structure.

In conclusion, a new type of substrate relaxation was revealed by the surface X-ray scattering study of CO adsorption on Pt(111), in which different layer expansions and in-plane rotations occur for the Pt atoms under the near-top-site and the near-bridge-site CO molecules. This observation demonstrates that subsurface atoms can move collectively forming a pattern on a nanometer scale determined by the unit cell of an adlayer. It also provides a possible explanation for why only one of the two geometrically allowed ($\sqrt{19}\times\sqrt{19}$)-13CO adlayer structures forms.

Acknowledgment. This work is supported by U.S. Department of Energy, Divisions of Chemical and Material Sciences, under the Contract No. DE-AC02-98CH10886 and at the Seitz Materials Research Laboratory under Contract No. DE-FG02-91ER45439.

References and Notes

(1) Fu, C. L.; Ho, K. M. *Phys. Rev. Lett*. **1989**, *63*, 1617.
(2) Wang, J.; Davenport, A. J.; Isaacs, H. S.; Ocko, B. M. *Science* **1992**, *255*, 1416.
(3) Haiss, W. *Rep. Prog. Phys*. **2001**, *65*, 591.
(4) Srivastava, G. P. *Comput. Phys. Commun*. **2001**, *137*, 143.
(5) Villegas, I.; Weaver, M. J. *J. Chem. Phys*. **1994**, *101*, 1648.
(6) Vestergaard, E. K.; Thostrup, P.; An, T.; Lagsgaard, E.; Stensgaard, I.; Hammer, B.; Besenbacher F. *Phys. Rev. Lett.* **2002**, *88*, 259601.
(7) Schuster, R.; Robinson, I. K.; Kuhnke K.; Kern, K. *Phys. Rev. B* **1996**, *54*, 17097.
(8) Lucas, C. A.; Markovic, N. M.; Ross, P. N. *Surf. Sci*. **1999**, *425*, L381.
(9) Feibelman, P. J.; Hammer, B.; Norskov, J. K.; Wagner, F.; Scheffler, M.; Stumpf, R.; Watwe, R.; Dumesic, J. *J. Phys. Chem. B* **2001**, *105*, 4018.
(10) Tolmachev, Y. V.; Menzel, A.; Tkachuk, A. V.; Chu, Y. S.; You, H. *Electrochem. And Solid-State Lett.* **2004**, *7*, E23.
(11) Wang, J. X.; Robinson, I. K.; Adzic, R. R. *Surf. Sci*. **1998**, *412/413*, 374.
(12) Lynch M.; Hu, P. *Surf. Sci*. **2000**, *458*, 1.
(13) Robinson, I. K.; Ferrer, S.; Torrellas, X.; Alvarez, J.; Silfhout, R. V.; Schuster, R.; Kuhnke, K.; Kern K. *Europhys. Lett.* **1995**, *32*, 37.
(14) Curulla, D.; Clotet, A.; Ricart, J. M.; Illas, F. *J. Phys. Chem. B* **1999**, *103*, 5246.